



Lightweight UV-C disinfection system

ROSEMARY C. SHE,¹ DONGYU CHEN,²  PIL PAK,¹ DENIZ K. ARMANI,³ ANDREAS SCHUBERT,³ AND ANDREA M. ARMANI^{2,4,*} 

¹Department of Pathology, Keck School of Medicine of the University of Southern California, Los Angeles, CA 90033, USA

²Ming Hsieh Department of Electrical Engineering, University of Southern California, Los Angeles, CA 90089, USA

³SMP Engineering, 1805 Flower Street, Glendale, CA 91201, USA

⁴Mork Family Department of Chemical Engineering and Materials Science, University of Southern California, Los Angeles, CA 90089, USA

*armani@usc.edu

Abstract: UV-C exposure is an effective disinfectant for a range of bacteria and viruses. As such, UV-C treatment, in combination with a chemical wipe, is a common cleaning protocol in medical facilities. Given the increase in severe bacterial and viral agents in society, having access to environmentally friendly disinfectant methods is of increasing interest. In response, we designed, constructed, and validated a UV-C disinfection system from readily accessible components. To improve the UV-C intensity, the enclosure interior was coated with chrome paint. The system is validated using *Bacillus cereus*, a gram-positive endospore-forming bacteria.

© 2020 Optical Society of America under the terms of the [OSA Open Access Publishing Agreement](#)

1. Introduction

Highly infectious microbial and viral diseases are a major challenge to global health, and, as such, are also a significant risk to global financial stability and security. While vaccines play a key role in preventing viral epidemics and pandemics, once an outbreak has occurred, the implementation of personal protective equipment (PPE) and disinfection measures to limit spread becomes paramount. Moreover, broadly applicable, yet environmentally friendly, disinfection methods play a key role beyond limiting the spread of viral agents. The number of antibiotic-resistant bacteria and fungi are rising every year. However, unlike in the past, the infections are originating “in the community”, not in healthcare settings [1]. Therefore, there is a need for easy to implement, broad-spectrum disinfection protocols.

To address this need, numerous methods of disinfection have been developed, including chemical (e.g. EPA hydrogen peroxide), radiation (ozone, UV-C, microwave), and thermal [2–7]. Among these different types, UV-C, also called UV germicidal irradiation (UVGI), disinfection has gained favor due to its efficacy against a broad range of microbial and viral agents in a variety of environments and on a wide range of surfaces [4,8,9].

The UV-C wavelength band covers 100nm–280nm, and it directly overlaps with the peak absorption of DNA and RNA (~260nm). The inactivation mechanism is straight-forward. Upon UV-C absorption, the pyrimidines in the RNA or DNA are converted to pyrimidine (6–4) pyrimidone photoproducts and cyclobutane pyrimidine dimers [10]. If the population of dimers is sufficiently high, transcription errors occur, ultimately resulting in inactivation of the bacteria or virus. As such, UV-C is a nearly universal disinfection method for bacteria, and its effectiveness in viral disinfection is not correlated with virus size, but with pyrimidine concentration.

Previous research efforts have shown 3 log inactivation of a range of viruses and bacteria using UV-C doses as low as 10mJ/cm² on non-porous surfaces [8–11]. However, this previous work relied on large commercial systems that can be challenging to procure, particularly in the midst of a pandemic or in a low resource environment. Thus, given the universality of UV-C as a disinfection method, in the face of the growing global personal protective equipment

shortage which directly impacts the safety of healthcare workers, researchers are investigating alternatives strategies of solving this immediate problem [12]. One approach relies on leveraging existing research biosafety cabinets. These systems have integrated UV-C disinfection systems that are designed to achieve the requisite doses, and thus, are ideally suited to be re-purposed as disinfection stations for both porous and non-porous materials [12]. However, a low-cost, portable solution would provide global benefit beyond the current challenge. Specifically, field-portable disinfection methods would aid in relief efforts during disasters as well as improve healthcare quality in low resource environments.

In this work, we demonstrate a home-built, portable UV-C disinfection system based on commonly available components, including a plastic bin, UV-C light bulb, and standard light housing (Fig. 1). To increase the UV-C intensity, the interior of the enclosure is coated with a reflective coating. Based on analytical calculations, the UV-C dose throughout the box should exceed $500\text{mJ}/\text{cm}^2$ with a 3 minute exposure. Using *Bacillus cereus* as a test organism and untreated plastic Petri dishes as a representative non-porous surface, the efficacy is experimentally validated. *B. cereus* is an aerobic, rod-shaped, gram-positive bacteria that can quickly multiply at room temperature. *B. cereus* can form endospores that can withstand harsh conditions including UV exposure [13,14]. Previous work demonstrated that a UV-C dose between $35\text{-}140\text{ mJ}/\text{cm}^2$ is required to achieve a 3 log reduction of *B. cereus* (vegetative) on non-porous surfaces [15,16].

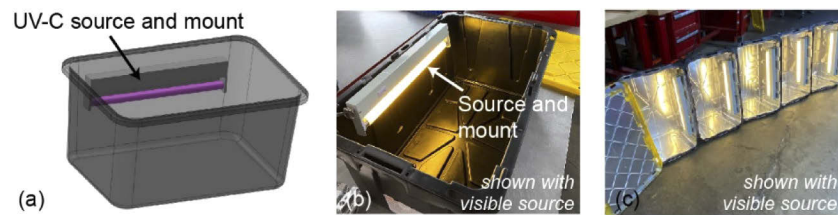


Fig. 1. UV-C Disinfection system. (a) Schematic of system. (b) Image of system before application of reflective coating, (c) Example of several systems on their sides. (Shown with visible lights for safety.)

2. Theory

The most important element of the system is optical power delivered by the UV-C source. As simple guidelines, the dose delivered by the UV-C source is dependent on the distance the object is away from the source, the source wattage and efficiency, and the exposure duration. In other words, a lower wattage source can be used in place of a higher wattage source, if the exposure duration is increased. Given that access to components may be highly variable, it is desirable to create a generalizable expression governing the UV-C intensity distribution inside of the UV-C system. This expression can then be used to calculate the impact of different bulbs on UV-C dose, accelerating re-design when needed.

As a starting point in creating the model, the UV-C bulb is treated like a linear light source, where each point on the bulb is a point light source with isotropic radiation. The cumulative UV-C dose created by the bulb is an integration of the dose generated by all the point light sources on the bulb. As is shown in Fig. 2, assuming we have an enclosure with length L , width W and height H . The bulb is placed on the side wall above the floor of the box by a height of h , and it has an optically active length of ℓ and is centered on the wall horizontally. Given this configuration, the location of any point source on the bulb can be expressed as $(X, 0, h)$, where $X \in \left[\frac{L-\ell}{2}, \frac{L+\ell}{2}\right]$. For any detection point (x, y, z) in the box, the distance between the point light

source and the detection point is:

$$Distance = \sqrt{(X - x)^2 + y^2 + (h - z)^2} \tag{1}$$

Assuming the UV-C wattage power of the bulb is P (unit: Watt), then the power of the point source is P/ℓ . As the point source radiates isotropically in a sphere, the radiation intensity on point (x, y, z) would be:

$$\frac{P/\ell}{4\pi ((X - x)^2 + y^2 + (h - z)^2)} \tag{2}$$

By integrating all the point sources on the bulb, we get the intensity generated by the whole bulb:

$$I = \int_{\frac{L-\ell}{2}}^{\frac{L+\ell}{2}} \frac{P/\ell * dX}{4\pi ((X - x)^2 + y^2 + (h - z)^2)} \tag{3}$$

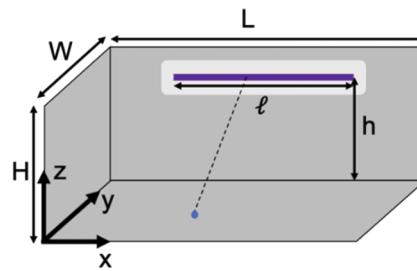


Fig. 2. Schematic showing key variables used to calculate cumulative UV-C dose.

The intensity calculated above is for the situation where there is no reflection from the box. However, in the system developed in the present work, the interior is coated with a reflective chrome paint. To simplify the reflection calculation and set a lower bound on the intensity inside the enclosure, we only take the first and second order of reflections into consideration. The calculation of intensity generated by the reflection is similar to the previous one with slight modifications. To account for the reflection, a series of “virtual light bulbs” with a power of αP for first order reflection and $\alpha^2 P$ for second order reflection, where α is the reflection rate, are located on virtual walls mirrored by other walls in the extended space. There are 6 first-order mirrored light sources and 30 second-order mirrored light sources in total. The intensity generated by each mirrored bulb can also be calculated using the integration method described above. The only difference is that the distance between point (x, y, z) and the mirrored bulb is different from the previous calculation. By adding the reflection caused by all the walls (including ceiling and floor) together, we get the intensity of the UV-C light inside the box. The intensity can be expressed in the following equation:

$$I_{with\ reflection} = \int_{\frac{L-\ell}{2}}^{\frac{L+\ell}{2}} \frac{P/l * dX}{4\pi((X - x)^2 + y^2 + (h - z)^2)} + \sum_{first-order\ reflection} \int_{\frac{L-\ell}{2}}^{\frac{L+\ell}{2}} \frac{\alpha P/l * dX}{New\ distance} + \sum_{second-order\ reflection} \int_{\frac{L-\ell}{2}}^{\frac{L+\ell}{2}} \frac{\alpha^2 P/l * dX}{New\ distance} \tag{4}$$

In the system shown in Fig. 1, $(L) = 78.74$ cm, $W = 50.8$ cm, $H = 35.56$ cm, $h = 25.4$ cm, and $\ell = 43.18$ cm. The wattage of the UV-C light bulb is 15 W, and, considering a 35% conversion efficiency, the UV-C wattage $P = 5.25$ W. By putting all these parameters into the equation, we

can calculate the intensity at any point in the box (unit: W/cm^2). To determine the UV-C dose, this value should be multiplied by the time that the system is on.

Figures 3(a)–3(c) shows the results from a series of calculations for an exposure time of 3 minutes. The wall reflectivity varies from 0% (Fig. 3(a)) to 85% (Fig. 3(c)). This represents the full range of possible values that could be achieved in the enclosure constructed as part of this work. The dose delivered varies by several orders of magnitude depending on the location within the enclosure and the reflectivity of the walls. Figure 3(d) shows the dose at the center of the enclosure from the very bottom to the top. As can be seen, even with modest wall reflectivity (25%), the enclosure is able to achieve doses above $10mJ/cm^2$ throughout this space, which is sufficient to meet guidelines for bacteria, and with reflectivities of 85%, doses well-above $100mJ/cm^2$ are reached, which is sufficient to meet guidelines for viruses.

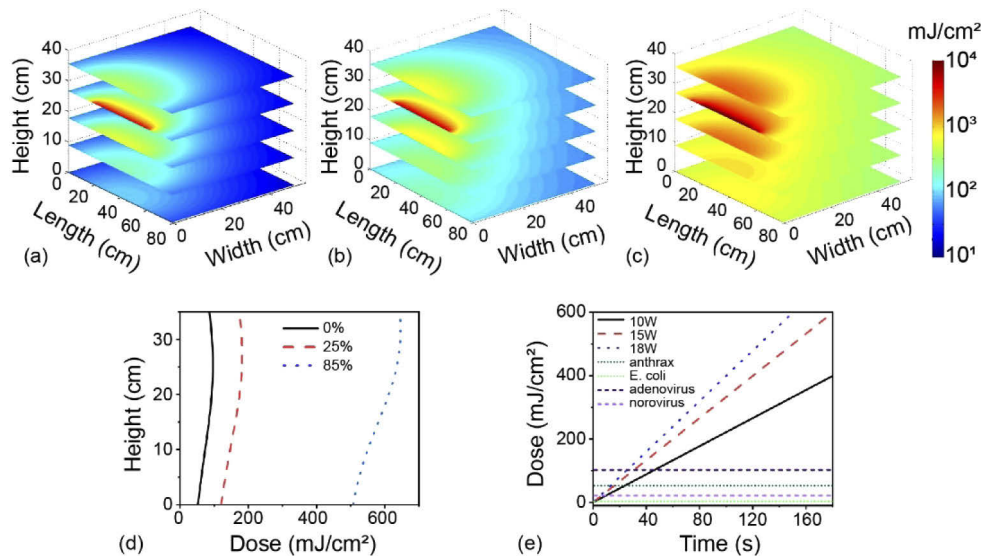


Fig. 3. Cumulative UV-C dose delivered for a three minute exposure inside the UV-C disinfection system. Three different wall reflectivity values are modeled: (a) 0%, (b) 25%, and (c) 85%. (d) The dose at different heights for all three reflectivities modeled, measured in the centered of the box x-y plane (e) Dose as a function of time for three different UV-C source powers. This calculation is performed at the center of the bottom of the enclosure. The specific coordinate based on the schematic in Fig. 2 is (39.4, 25.4, 0). For comparison, the requisite doses to achieve three log reduction in growth for two bacteria and two viruses are also plotted [17–20].

To compare the effects of the power generated by different optical sources, the calculation was run with two additional sources with lower and higher powers, and the dose in the bottom-center of the box was determined for different exposure times. As can be observed in Fig. 3(e), with a higher power source, the exposure duration needed to achieve a specific dose depended linearly on optical power. For context, the doses required to achieve three log reduction of two bacteria and two viruses are included in Fig. 3(e) [17–20]. However, it is critical to note that this calculation does not consider thermal effects. For example, if high enough powers are used with optically absorbing materials, some optical power will be lost to thermal heating. Thermal heating is particularly deleterious when the system is being used for PPE re-use as it can result in the degradation of the PPE.

3. Experimental methods and results

The UV-C disinfection system is comprised of two basic components: an enclosure with a reflective interior and a UV-C source. To build the enclosure, the interior of a 17 gallon tote (Home Depot) was first cleaned with Acetone and then coated with chrome spray-paint (Rustoleum, Bright coat Metallic Chrome, Home Depot). This chrome spray paint is primarily comprised of aluminum which has up to 90% reflectivity in the UV-C wavelength range [21]. The UV-C source was an 18" Philips UV-C bulb (G-15T8, 15W, McMaster). This low pressure mercury bulb designed for UV-C disinfection has a primary emission at 254nm. Two holes were drilled in the side of the tote to mount an under-counter light fixture (Home Depot) which held the UV-C source. Power was supplied to the light fixture via a power cord which was run through a third hole, located in the corner. To control the light externally, the power cord was plugged into a power strip with an on/off switch. Based on this part list from these vendors at this time, the entire materials cost of building one system was approximately \$72.00.

B. cereus previously isolated from routine clinical culture was selected for this study. After subculture on sheep blood agar and overnight incubation at 35°C, a 4.0 McFarland suspension was prepared in sterile 0.45% saline solution. For analysis of UV-C irradiation of plastic surface, 100 µL aliquots were dispensed onto sterile polystyrene Petri dishes (100 mm diameter) to mimic face shield surfaces over an approximately 1 × 2 cm area, then allowed to completely dry at 35°C, up to 30 minutes. Exposure times of 1, 3, and 6 minutes were tested as well as control (no exposure) measurements. Three replicates were included for each exposure time at three different locations equally spaced on the bottom of the box ($z=0$), including one in the center, as modelled in Fig. 3(e), and one on either side (19.7, 25.4, 0) and (59.1, 25.4, 0).

Immediately after the UV-C radiation treatment, each Petri dish was flooded with 10 mL of 0.45% saline and scraped to completely resuspend the film. For baseline counts, 100 µL of 1:100 and 1:10,000 dilutions were plated on sheep blood agar in duplicate. For UV-C irradiated organism counts, 100 µL of neat, 1:100, and 1:10,000 dilutions of each sample were plated in duplicate. After a 24 hr incubation of culture plates at 35°C in 5% CO₂, individual colonies were enumerated and the dilution resulting in the highest calculated mean organism concentration was used for analysis.

For analysis of direct irradiation of agar media, sheep blood agar plates were inoculated with 1 µL and 10 µL of the 4.0 McF suspension prior to UV-C exposure. Baseline counts were obtained for each experiment and were prepared in the same manner as experimental samples.

As can be seen in Fig. 4(a), the *B. cereus* samples that were not exposed to UV-C readily formed colonies after 24 hour incubation time indicating that all preparation methods were correct. The baseline counts of Petri dish organism films ranged from 1 to 3 × 10⁶ colony forming units (CFU). In contrast, this growth was dramatically eliminated when the samples were exposed to the UV-C, even with only 1 minute exposure (Fig. 4(a)).

At 1 minute of UV-C exposure, all organism counts were nil except for one of three replicates in which 800 CFU remained. At 3 and 6 minute UV-C exposure times, organism counts were reduced to undetectable levels except for one of three replicates in which 100 CFU remained. Directly irradiated organisms on blood agar plates demonstrated no growth of organisms at 3 and 6 minute exposure times but growth of 700 CFU/mL after 1 minute exposure, whereas baseline count was >3 × 10⁵ CFU/mL (Figs. 4(b) and 4(c)). As mentioned, previous work demonstrated that a dose between 35-140 mJ/cm² of UV-C achieved a 3 log reduction of vegetative *B. cereus* cells. Based on the analytical calculations presented in Fig. 3(e), (a) 1 minute exposure in the center of the box should have provided a dose in excess of 200mJ/cm². Therefore, these findings align with the prior results [15,16].

In addition to achieving >3 log reduction, the exposure times compare favorably to commercial UV-C disinfection systems which typically have disinfection protocols between 1-2 minutes. The alignment between the current portable, lightweight approach and the conventional commercial

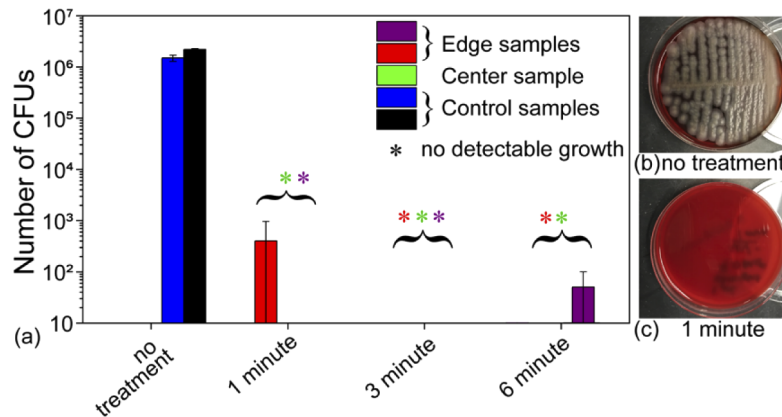


Fig. 4. Summary of results. (a) In both control samples, over 10^6 colony forming units (CFUs) grew during the 24 hour incubation period. In contrast, the majority of the exposed dishes were unable to support colony formation, indicating a 6 log reduction. (b) Control sample of *B. cereus* not exposed to UV-C formed colonies after 24 hour incubation time. (c) In contrast, this growth was dramatically eliminated after 1 minute exposure of identical sample preparations to the UV-C.

systems is possible because the cumulative dose delivered is the same, as shown in Fig. 3. However, the proposed system offers numerous advantages. Specifically, the design can be adapted to use any UV-C bulb length, it is easy to construct, and it is less expensive.

4. Conclusions

In conclusion, we have designed and validated a simple to construct UV-C disinfection system. It uses readily available, inexpensive components to create the UV-C chamber. The efficiency of the system is further improved by coating the interior with a reflective material. As a result, the intensity of the UV-C optical field is amplified, allowing shorter exposure times to be used. Over 3 log reduction in CFUs on a polystyrene (or non-porous) surface is confirmed using *B. cereus* as a model bacteria. Future research efforts are focused on improving the operational safety of the system by integrating pressure switches to automatically control the UV-C source, on exploring alternative light sources, such as UV-C LEDs, to improve the robustness and power management, and on optimizing UV-C for porous media disinfection, notably mask re-use. This approach will find use during the current COVID-19 pandemic where PPE, such as faceshields and masks, is in short supply as well as in the future in low resource environments [22].

Funding

National Science Foundation (2028445); Army Research Office (W911NF1810033).

Acknowledgements

The authors would like to thank Dr. Kimberly Lengyel and Dr. Neha Nanda for their advice on system design and Dr. Hyungwoo Choi for assistance on preparing a rendering.

Disclosures

The authors declare no conflicts of interest.

References

1. Centers for Disease Control and Prevention (U.S.), *Antibiotic Resistance Threats in the United States, 2019* (Centers for Disease Control and Prevention (U.S.), 2019).
2. W. Rutala and D. Weber, "Uses of inorganic hypochlorite (bleach) in health-care facilities," *Clin. Microbiol. Rev.* **10**(4), 597–610 (1997).
3. W. Cochran, G. McFeters, and P. Stewart, "Reduced susceptibility of thin *Pseudomonas aeruginosa* biofilms to hydrogen peroxide and monochloramine," *J. Appl. Microbiol.* **88**(1), 22–30 (2001).
4. J. Koivunen and H. Heinonen-Tanski, "Inactivation of enteric microorganisms with chemical disinfectants, UV irradiation and combined chemical/UV treatments," *Water Res.* **39**(8), 1519–1526 (2005).
5. M. Berney, H. Weilenmann, J. Ihssen, C. Bassin, and T. Egli, "Specific growth rate determines the sensitivity of *Escherichia coli* to thermal, UVA, and solar disinfection," *Appl. Environ. Microbiol.* **72**(4), 2586–2593 (2006).
6. A. Kramer, I. Schwebke, and G. Kampf, "How long do nosocomial pathogens persist on inanimate surfaces? A systematic review," *BMC Infect. Dis.* **6**(1), 130 (2006).
7. P. Setlow, "Spores of *Bacillus subtilis*: their resistance to and killing by radiation, heat and chemicals," *J. Appl. Microbiol.* **101**(3), 514–525 (2006).
8. K. Bergmann, "UV-C Irradiation: A New Viral Inactivation Method for Biopharmaceuticals," *American Pharmaceutical Review* (2014).
9. W. Hijnen, E. Beerendonk, and G. Medema, "Inactivation credit of UV radiation for viruses, bacteria and protozoan (oo)cysts in water: A review," *Water Res.* **40**(1), 3–22 (2006).
10. R. Sinha and D. Hader, "UV-induced DNA damage and repair: a review," *Photochem. Photobiol. Sci.* **1**(4), 225–236 (2002).
11. FDA, *CFR - Code of Federal Regulations Title 21*, Code of Federal Regulations Title 21 (US Government, 2019), Vol. 8.
12. K. J. Card, D. Crozier, A. Dhawan, M. Dinh, E. Dolson, N. Farrokhan, V. Gopalakrishnan, E. Ho, E. S. King, N. Krishnan, G. Kuzmin, J. Maltas, J. Pelesko, J. A. Scarborough, J. G. Scott, G. Sedor, and D. T. Weaver, "UV Sterilization of Personal Protective Equipment with Idle Laboratory Biosafety Cabinets During the Covid-19 Pandemic," medRxiv (2020).
13. A. Soni, I. Oey, P. Silcock, and P. Bremer, "Bacillus Spores in the Food Industry: A Review on Resistance and Response to Novel Inactivation Technologies," *Compr. Rev. Food Sci. Food Saf.* **15**(6), 1139–1148 (2016).
14. P. Setlow, "Resistance of spores of *Bacillus* species to ultraviolet light," *Environ. Mol. Mutagen.* **38**(2-3), 97–104 (2001).
15. M. Clauß, "Higher effectiveness of photoinactivation of bacterial spores, UV resistant vegetative bacteria and mold spores with 222 nm compared to 254 nm wavelength," *Acta Hydrochim. Hydrobiol.* **34**(6), 525–532 (2006).
16. B. Ernest R., M. Anne, A. Arthur I., and B. Lindsay, "Inactivation of *Bacillus* Spores by Ultraviolet or Gamma Radiation," *J. Environ. Eng.* **131**(9), 1245–1252 (2005).
17. W. L. Nicholson and B. Galeano, "UV Resistance of *Bacillus anthracis* Spores Revisited: Validation of *Bacillus subtilis* Spores as UV Surrogates for Spores of *B. anthracis* Sterne," *Appl. Environ. Microbiol.* **69**(2), 1327–1330 (2003).
18. G. D. Harris, V. D. Adams, D. L. Sorensen, and M. S. Curtis, "Ultraviolet inactivation of selected bacteria and viruses with photoreactivation of the bacteria," *Water Res.* **21**(6), 687–692 (1987).
19. N. Nwachuku, C. P. Gerba, A. Oswald, and F. D. Mashadi, "Comparative inactivation of adenovirus serotypes by UV light disinfection," *Appl. Environ. Microbiol.* **71**(9), 5633–5636 (2005).
20. J. Lee, K. Zoh, and G. Ko, "Inactivation and UV disinfection of murine norovirus with TiO₂ under various environmental conditions," *Appl. Environ. Microbiol.* **74**(7), 2111–2117 (2008).
21. J. Edmends, C. Maldé, and S. Corrigan, "Measurements of the far ultraviolet reflectivity of evaporated aluminum films under exposure to O₂, H₂O, CO and CO₂," *Vacuum* **40**(5), 471–475 (1990).
22. A. M. Armani, D. E. Hurt, D. Hwang, M. C. McCarthy, and A. Scholtz, "Low-tech solutions for the COVID-19 supply chain crisis," *Nat. Rev. Mater.* **5**(6), 403–406 (2020).